Sci. Technol. Adv. Mater. **12** (2011) 034402 (6pp) doi:10.1088/1468-6996/12/3/034402

# Mechanochemically synthesized $CsH_2PO_4$–$H_3PW_{12}O_{40}$ composites as proton-conducting electrolytes for fuel cell systems in a dry atmosphere

**Song-yul Oh[1], Evan K Insani[1,2], Van H Nguyen[1], Go Kawamura[3], Hiroyuki Muto[1,3], Mototsugu Sakai[3] and Atsunori Matsuda[1,3]**

[1] Department of Environmental and Life Sciences, Toyohashi University of Technology, Tempaku-cho, Toyohashi, Aichi 441-8580, Japan
[2] Department of Engineering Physics, Institute Technology of Bandung, Jl. Ganesha 10, Bandung 40132, Indonesia
[3] Department of Electrical and Electronic Information Engineering, Toyohashi University of Technology, Tempaku-cho, Toyohashi, Aichi 441-8580, Japan

E-mail: matsuda@ee.tut.ac.jp

Received 4 October 2010
Accepted for publication 6 February 2011
Published 3 May 2011
Online at stacks.iop.org/STAM/12/034402

**Abstract**
Cesium dihydrogen phosphate ($CsH_2PO_4$, CDP) and dodecaphosphotungstic acid ($H_3PW_{12}O_{40}{\cdot}nH_2O$, WPA$\cdot nH_2O$) were mechanochemically milled to synthesize CDP–WPA composites. The ionic conductivities of these composites were measured by an ac impedance method under anhydrous conditions. Despite the synthesis temperatures being much lower than the dehydration and phase-transition temperatures of CDP under anhydrous conditions, the ionic conductivities of the studied composites increased significantly. The highest ionic conductivity of $6.58 \times 10^{-4}$ Scm$^{-1}$ was achieved for the 95CDP·5WPA composite electrolyte at 170 °C under anhydrous conditions. The ionic conduction was probably induced in the percolated interfacial phase between CDP and WPA. The phenomenon of high ionic conduction differs for the CDP–WPA composite and pure CDP or pure WPA under anhydrous conditions. The newly developed hydrogen interaction between CDP and WPA supports anhydrous proton conduction in the composites.

Keywords: dry fuel cell, inorganic solid acid, cesium dihydrogen phosphate, phosphotungstic acid, advanced composite

## 1. Introduction

Inorganic solid acids, such as sulfates and phosphates, have been widely studied for their application in proton exchange fuel cells because of their high proton conductivities and phase transition to superprotonic states [1–3]. Among the inorganic solid acids under active development, cesium dihydrogen phosphate ($CsH_2PO_4$, CDP) has attracted much attention owing to its ability to maintain high proton conductivity at temperatures above 230 °C, at which temperature it transforms from a monoclinic to a tetragonal structure. It has also shown promising fuel cell performance in both hydrogen and direct alcohol systems [4–6]. However, CDP retains its thermally stable superprotonic phase only under hydrous condition, for example, in a gaseous 30 mol.% $H_2O$/Ar mixture [7]. While CDP should be heated to above 230 °C to induce high conductivity, it dehydrates and decomposes into metaphosphate ($CsPO_3$) at temperatures above 200 °C [8]. This dehydration can be suppressed by maintaining sufficient humidity in the fuel cell systems, but it becomes a problem when scaling up the system.

 

In contrast, partly $Cs^+$-substituted heteropoly acids (Cs-HPAs) have attracted significant attention owing to their higher catalytic activity with better chemical stabilities than pristine HPAs in many acid-type reactions [9]. Such Cs-HPAs are generally prepared by precipitation from aqueous solutions [10, 11]. On the other hand, we have shown that a solid-state reaction involving mechanochemical treatment using a high-energy ball mill is a promising method of improving the proton conductivity of inorganic solid acids and of synthesizing a new class of inorganic solid acid-based composites [12, 13]. When mixtures of cesium hydrogen sulfate ($CsHSO_4$, CHS) and phosphotungstic acid ($H_3PW_{12}O_{40}$, WPA) were mechanochemically milled, $Cs_xH_{3-x}PW_{12}O_{40}$ was formed, which shows proton conductivity two to five orders of magnitude higher than that of the raw substances under anhydrous condition.

Recently, it has been reported that the proton conductivity of CDP is increased by introducing silica nanoparticles, especially at temperatures below the phase-transition temperature under hydrous condition [7, 14, 15]. However, high proton conductivity of CDP under anhydrous condition has not been reported to the best of our knowledge. In this study, CDP and WPA were mechanochemically milled to obtain CDP–WPA composites, aiming to produce electrolytes with high proton conductivity over a wide temperature range and under anhydrous condition for application to fuel cells. The CDP–WPA composites were characterized in term of their thermal stability and structural and electrochemical properties.

## 2. Experimental details

Reagent-grade $CsH_2PO_4$ (CDP) and $H_3PW_{12}O_{40}{\cdot}nH_2O$ (WPA$\cdot nH_2O$) were purchased from Soekawa Chemical Co. Ltd and Wako Pure Chemical Industries, respectively, and used as starting materials for the synthesis of various CDP–WPA composites. Prior to mechanochemical milling, WPA$\cdot nH_2O$ was kept at 60 °C for about a day to remove the physisorbed water and obtain WPA$\cdot 6H_2O$.

The mechanochemical milling of $CsH_2PO_4$ and WPA$\cdot 6H_2O$ was carried out for various compositions, in dry nitrogen atmosphere, using a planetary ball mill (Fritsch Pulverisette 7). Agate was selected as the material for the pot and the ball. The rotation speeds of the milling pot and table were maintained at 720 rpm with a constant rotation ratio of 1 : 1, and the milling was carried out for 10 min. The volume of the pot was 45 ml and 10 balls of 10 mm diameter were used for the milling. The sample weight was fixed at 2.0 g. Composites with the ratio $x$CDP$\cdot(100-x)$WPA were prepared, where $x$ was varied between 50 and 95 mol.%.

Powder x-ray diffraction (XRD; Ultima IV, Rigaku) patterns of the mechanochemically milled $x$CDP$\cdot(100-x)$ WPA composite powders were recorded at room temperature (RT) using a Cu $K_\alpha$ radiation source.

Fourier transform Raman (FT Raman; NRS-3100, Jasco) spectra were measured in the range of 115–1220 $cm^{-1}$, using a 532 nm laser for excitation and a concave glass substrate. Fourier transform infrared (FTIR; 3100 FT-IR, Varian) spectra were recorded between 400 and 4000 $cm^{-1}$ using KBr pellets.

Differential scanning calorimetry (DSC; Thermo plus DSC 8230, Rigaku) was carried out to determine the phase-transition behavior of CDP–WPA composites. The samples were heated from RT to 300 °C at a rate of 10 °C $min^{-1}$ in air.

The temperature dependence of powder XRD patterns was studied using *in situ* XRD-DSC (Ultima IV-Thermoplus EVO II, Rigaku) technique in dry nitrogen atmosphere. The XRD pattern was scanned between 20 and 30° at a rate of 2° $min^{-1}$, and the temperature was varied between 50 and 180 °C at a rate of 2 °C $min^{-1}$ for 3 cycles.

Solid proton magic-angle-spinning nuclear magnetic resonance ($^1$H MAS NMR; UNITY-400P, VARIAN) measurements were carried out at RT using a typical single pulse sequence. The sample spinning rate was 5 kHz. The frequency scale was calibrated using neat tetramethylsilane (TMS) after adjusting the signal of adamantine spinning at 8.0 kHz to 1.87 parts per million (ppm). Sample powders for the MAS NMR measurements were dried at 170 °C in vacuum for 3 h and filled into a MAS rotor in dry nitrogen atmosphere.

Proton conductivity of the CDP–WPA composite was evaluated by ac impedance spectroscopy over a frequency range of 1–$10^7$ Hz using SI 1260-based system (Solartron). For proton conductivity measurement, pellets (13 mm in diameter) were prepared by pressing the synthesized composite powders at 60 MPa for 10 min. Before the compression, carbon sheets were placed on both sides of the composite powder to form electrodes. The proton conductivity, $\sigma$, of the sample was calculated from the impedance data as $\sigma = d/RS$, where $d$ and $S$ are the thickness and face area of the sample, respectively. $R$ was derived from the low intersect of the high-frequency semicircle on the complex impedance plane with the real Re($Z$) axis. For each set of measurement conditions, all composite electrolytes were equilibrated for 1 h before measuring the conductivity.

## 3. Results and discussion

Figure 1 shows powder XRD patterns of various $x$CDP$\cdot(100-x)$WPA composites. The diffraction peaks of CDP (topmost in figure 1) and WPA$\cdot 6H_2O$ (bottom) were obvious before milling, whereas after milling for 10 min, large changes were observed in the XRD patterns around 25–26°. The diffraction peak at 25.5° with the highest intensity for WPA shifted to higher angles in the composites, indicating that $H^+$ ion in WPA was partly substituted with $Cs^+$ ion to form $Cs_xH_{3-x}PW_{12}O_{40}$ upon mechanochemical milling. The XRD patterns of the composites are quite different from those of CDP. For CDP, a monoclinic phase was observed with the main peak at 23.7°. Most peaks in CDP-WPA composites can be assigned to WPA, and the main peak of CDP appears in the composites with $x = 90$ and 95. This result suggests a decrease in the interplanar spacing (d) of the Keggin unit of WPA for these composites owing to the electrostatic

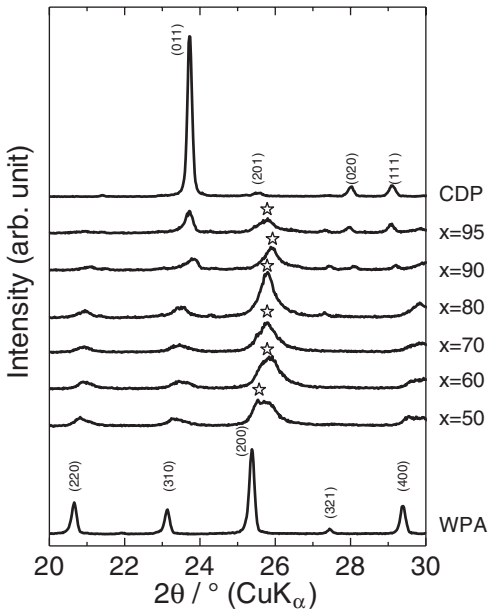


**Figure 1.** Powder XRD patterns of CDP, WPA and mechanochemically milled $x$CDP·$(100-x)$WPA composites (720 rpm for 10 min in dry nitrogen atmosphere).

compaction induced by the introduction of large $Cs^+$ cations into WPA [16, 17].

Structural changes in the $x$CDP·$(100-x)$WPA composites were also observed by FT Raman and FTIR spectroscopies. Intense bands in the FT Raman spectrum of WPA (figure 2) at 211 and 1003 $cm^{-1}$ were assigned to W–$O_{bc}$ (corner- and edge-shared W–O–W) and W═$O_d$ (terminal W═O) modes, respectively. Upon milling of CDP with WPA, the W–$O_{bc}$ Raman band was not changed, whereas the W═$O_d$ band shifted significantly to high frequencies with increasing $x$. These features were clarified in the FTIR spectra in figure 3. Bands at 786, 885, 976 and 1080 $cm^{-1}$ are attributed to W–$O_c$ (edge-shared W–O–W), W–$O_b$ (corner-shared W–O–W), W═$O_d$ (terminal W═O) and P–$O_a$ vibrations in WPA, respectively [18]. The W═$O_d$ IR band shifted significantly to high frequency, especially for $x \geqslant 80$, which is similar to the Raman results. These observations indicate shortening of the W═$O_d$ bond in WPA for these composites owing to the electrostatic compaction induced by introducing relatively large $Cs^+$ cations into WPA.

We have already reported similar changes in the crystalline and chemical structures of mechanochemically synthesized CHS–WPA composites [16, 17]. Although the $Cs^+$ ion source of CHS–WPA systems is clearly different from that in this study, both composite systems showed very similar changes in diffraction patterns, especially a shift of the main peak of WPA to a higher angle compared with that of pure WPA. These observations imply that a solid-state reaction induced by mechanochemical treatment is a promising method of synthesizing a new class of inorganic solid acid-based composites.

The thermal properties of CDP and $x$CDP·$(100-x)$WPA composites were evaluated by DSC as shown in figure 4.

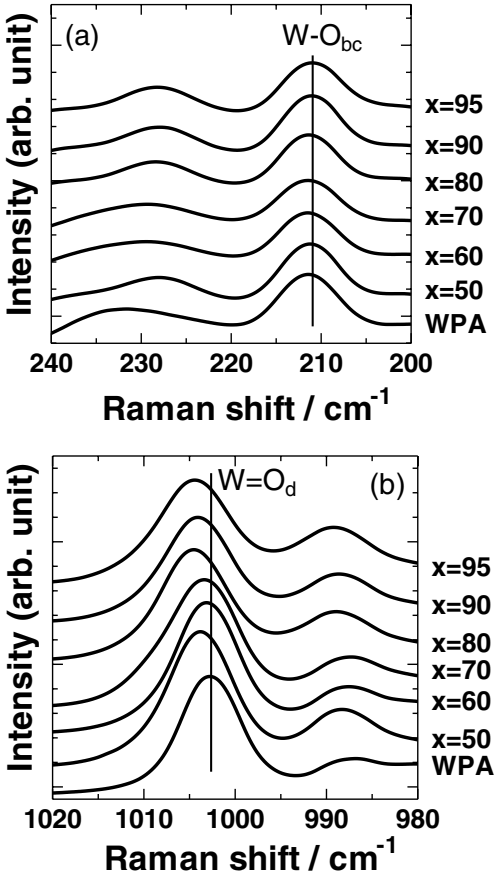


**Figure 2.** FT Raman spectra of WPA and mechanochemically milled $x$CDP·$(100-x)$WPA composites.

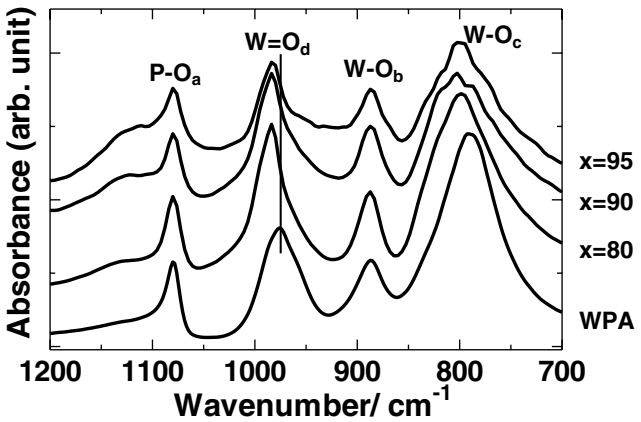


**Figure 3.** FTIR absorption spectra of WPA and mechanochemically milled $x$CDP·$(100-x)$WPA composites.

A significant endothermic peak was observed at 235 °C for pure CDP in dry nitrogen atmosphere and associated with the dehydration of CDP. The DSC spectrum changed significantly for composite systems: after mechanochemical milling, the dehydration peak of CDP split, broadened and shifted to lower temperatures with decreasing $x$; it almost disappeared for the composites with $x \leqslant 80$. These observations imply the formation of a disordered state in composites due to the chemical interaction between CDP and WPA induced by mechanochemical milling [14].

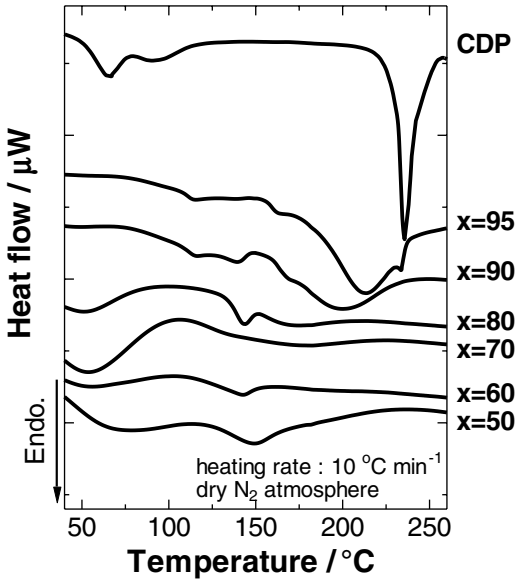


**Figure 4.** DSC curves of CDP and mechanochemically milled $x$CDP·$(100-x)$WPA composites measured in dry nitrogen atmosphere.

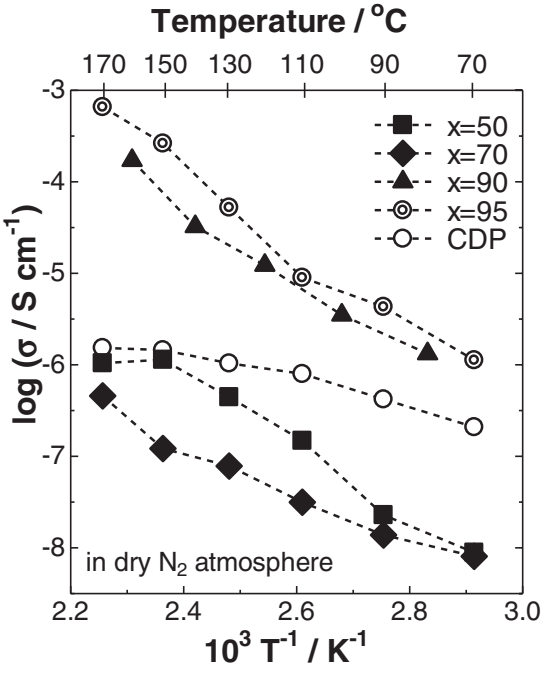


**Figure 5.** Temperature dependence of conductivity of $x$CDP·$(100-x)$WPA composites in dry nitrogen atmosphere.

Changes in the proton conductivity of the $x$CDP·$(100-x)$WPA composites were measured on cooling from 170 to 70 °C, which is below the dehydration and phase-transition temperatures of CDP. Figure 5 shows proton conductivity as a function of temperature for $x$CDP·$(100-x)$WPA composites in dry nitrogen atmosphere. The ionic conductivity of CDP was changed markedly with the addition of WPA, and the highest ionic conductivity of $6.58\times10^{-4}$ Scm$^{-1}$ was achieved for the 95CDP·5WPA composite electrolyte at 170 °C in dry nitrogen atmosphere. It is noteworthy that

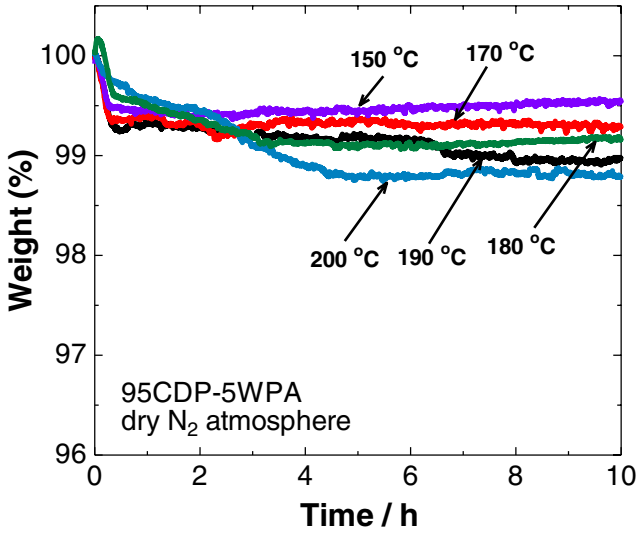


**Figure 6.** Thermal stability of 95CDP·5WPA composite at different temperatures in dry nitrogen atmosphere.

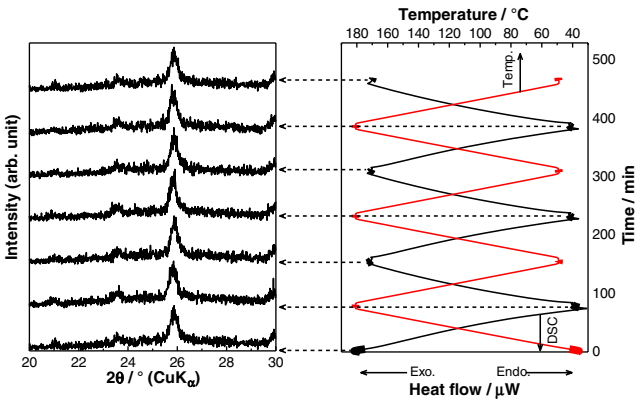


**Figure 7.** XRD–DSC patterns of 95CDP·5WPA composite in a temperature range of 50–180 °C in dry nitrogen atmosphere.

the CDP composite electrolyte containing a small amount of WPA has conductivity one to three orders of magnitude higher than that of pure CDP under anhydrous condition. This increase is probably related to not only the wetting of CDP by hydrate in WPA but also the newly formed hydrogen bonds between CDP and WPA. On the other hand, the ionic conductivity is lower in composite electrolytes with $x \leqslant 70$ than in CDP. Probably the high WPA content acted as a barrier for proton transfer and hindered ionic conduction via the so-called 'geometrical effect' [19, 20].

The thermal stability was evaluated in dry nitrogen atmosphere for 95CDP·5WPA composite (figure 6) and was acceptable up to 180 °C for 10 h. A slight weight loss (about 0.2 wt.%) occurred at 190 °C after the evaporation of adsorbed water, and a considerable weight loss due to dehydration of the composite was observed at 200 °C. The corresponding powder XRD pattern (figure 7) was unchanged between 50 and 180 °C in dry nitrogen atmosphere for 3 cycles, revealing the lack of structural changes in this temperature range. The proton conductivity of the 95CDP·5WPA composite in dry nitrogen atmosphere was studied between 50 and 170 °C for 3 cycles (figure 8). A small hysteresis was observed and attributed

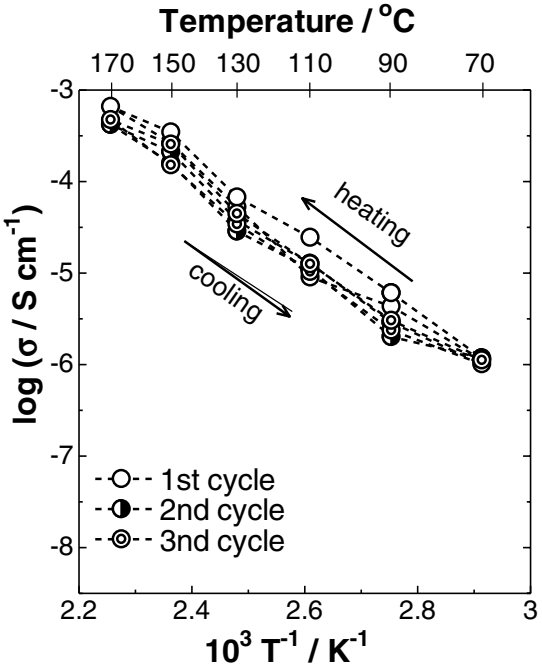


**Figure 8.** Temperature dependences of proton conductivity of 95CDP·5WPA composite for 3 cycles in dry nitrogen atmosphere.

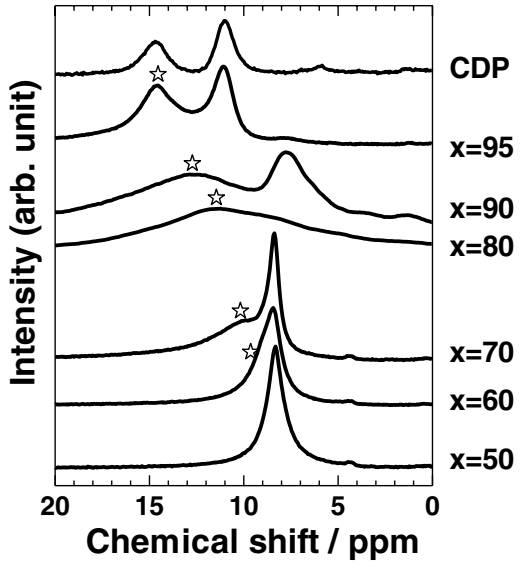


**Figure 9.** $^1$H NMR spectra of $x$CDP·$(100-x)$WPA composites.

to the dissimilar initial conditions for various cycles—the conductivity was slightly higher in the first cycle due to the physisorbed water. From the thermal analyses, we expect that the high proton conductivity of 95CDP·5WPA composite can long be maintained at temperatures up to 180 °C under anhydrous condition.

Figure 9 shows the $^1$H MAS NMR spectra of mechanochemically milled $x$CDP·$(100-x)$WPA composites. All the samples were dried at 170 °C in vacuum for 3 h to remove adsorbed water prior to the measurements. Two broad signals are observed for pure CDP at 11.04 and 14.70 ppm and can be ascribed to mobile protons in CDP. After mechanochemical milling, the signals progressively shifted

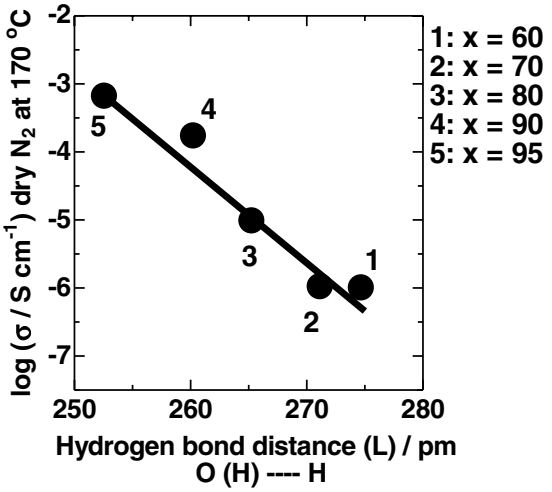


**Figure 10.** Relationship between hydrogen bond distance ($L$) and proton conductivity at 170 °C in dry $N_2$ atmosphere for $x$CDP·$(100-x)$WPA composites; $L$ was calculated as $L = 100 \times (79.05 - \delta_{iso})/25.5$, where $\delta_{iso}$ is the $^1$H chemical shift (denoted by ☆ in figure 9).

to lower magnetic fields with increasing $x$ indicating a higher hydrogen bonding strength [21]. From these results, the hydrogen bonding distance ($L$) between OH in CDP and $O_d$ in WPA was estimated using the relation $L = 100 \times (79.05 - \delta_{iso})/25.5$, where $\delta_{iso}$ is the $^1$H chemical shift (denoted by ☆) expressed in ppm with respect to the TMS signal [22, 23]. Figure 10 shows the relationship for $x$CDP·$(100-x)$WPA composites between $L$ and proton conductivity in dry nitrogen atmosphere at 170 °C, i.e. below the dehydration and phase-transition temperatures of CDP. For the mechanochemically milled CDP–WPA composite system, the proton conductivity in dry nitrogen atmosphere showed a good correlation with the hydrogen bond distance (O(H) ... H). Thus, the shortening of the hydrogen bond distance affects the proton conductivity of the CDP–WPA composites.

Previously, we found that the mechanochemically synthesized CHS–WPA composites exhibit high proton conductivity under anhydrous condition, and better water stability than their raw substances [16, 17]. Nevertheless, the catalyzed reduction of sulfate solid acids under hydrogen atmosphere may degrade the electrochemical performance during fuel cell operation [24]. On the other hand, CDP requires a certain level of humidity to achieve high proton conductivity, whereas the phosphate solid acid is not reduced to form solid phosphorus or gaseous $H_xP$ species [4]. Therefore, improvement of proton conductivity of CDP under anhydrous condition is important for fuel cell design.

In this study, the CDP–WPA composites consisted of a bulky phase and an interfacial phase. XRD and spectral results suggest that a disordered CDP structure was produced at the surface and/or inside of WPA particles. This well-dispersed disordered CDP phase can form ionic percolation pathways via the interfacial phase. Even at much lower temperatures than the dehydration and phase-transition temperatures of CDP under anhydrous condition, the ionic percolation can

be induced in such interfacial phase, improving protonic conduction. This phenomenon is superior to the protonic conduction behavior of pure CDP under anhydrous condition, especially at low temperatures.

## 4. Conclusions

Solid acid $x$CDP·$(100-x)$WPA composites were synthesized by mechanochemical milling. The powder XRD patterns and spectral measurements indicated that the $H^+$ ions in WPA were partly substituted by $Cs^+$ cations with relatively large ionic radius to form $Cs_xH_{3-x}PW_{12}O_{40}$ owing to the compaction by mechanochemical milling. The protonic conductivity under anhydrous condition was improved at temperatures lower than the dehydration and phase-transition temperatures of pure CDP. Ionic percolation for composite systems will be induced in the interfacial phase between CDP and WPA, improving protonic conduction. Mechanochemically synthesized CDP–WPA composite electrolytes are superior to pure CDP or WPA.

## Acknowledgment

This work was partly supported by the Ministry of Education, Culture, Sports, Science, and Technology of Japan (Grant-in-Aid for Scientific Research on Priority Areas No. 439 'Nanoionics,' A02 No. 19017009), by the Japan Society for the Promotion of Science (Challenging Exploratory Research No. 21655075) and by The Murata Science Foundation.

## References

[1] Baranov A I, Shuvalov L A and Shchagina N M 1982 *JETP Lett.* **36** 459
[2] Norby T 1999 *Solid State Ion.* **125** 1
[3] Suwa Y, Yamauchi J, Kageshima H and Tsuneyuki S 2001 *Mater. Sci. Eng.* B **79** 31
[4] Boysen D A, Uda T, Chisholm C R I and Haile S M 2004 *Science* **303** 68
[5] Uda T and Haile S M 2005 *Electrochem. Solid-State Lett.* **8** A245
[6] Uda T, Boysen D A, Chisholm C R I and Haile S M 2006 *Electrochem. Solid-State Lett.* **9** A261
[7] Otomo J, Minagawa N, Wen C J, Eguchi K and Takahashi H 2003 *Solid State Ion.* **156** 357
[8] Taninouchi Y, Uda T, Awakura Y, Ikeda A and Haile S M 2007 *J. Mater. Chem.* **17** 3182
[9] Okuhara T, Mizuno N and Misono M 1996 *Adv. Catal.* **41** 113
[10] Okuhara T, Watanabe H, Nishimura T, Inumaru K and Misono M 2000 *Chem. Mater.* **12** 2230
[11] Narasimharao K, Brown D R, Lee A F, Newman A D, Siril P F, Tavener S J and Wilson K 2007 *J. Catal.* **248** 226
[12] Matsuda A, Tezuka T, Nono Y, Tadanaga K, Minami T and Tatsumisago M 2005 *Solid State Ion.* **176** 2899
[13] Matsuda A, Kikuchi T, Katagiri K, Muto H and Sakai M 2006 *Solid State Ion.* **177** 2421
[14] Ponomareva V G and Shutova E S 2007 *Solid State Ion.* **178** 729
[15] Otomo J, Ishigooka T, Kitano T, Takahashi H and Nagamoto H 2008 *Electrochim. Acta* **53** 8186
[16] Matsuda A, Kikuchi T, Katagiri K, Daiko Y, Muto H and Sakai M 2007 *Solid State Ion.* **178** 723
[17] Daiko Y, Takagi H, Katagiri K, Muto H, Sakai M and Matsuda A 2008 *Solid State Ion.* **179** 1174
[18] Kim Y S, Wang F, Hickner M, Zawodzinski T A and McGrath J E 2003 *J. Membr. Sci.* **212** 263
[19] Kreuer K D 1996 *Chem. Mater.* **8** 610
[20] Kreuer K D, Fuchs A, Ise M, Spaeth M and Maier J 1998 *Electrochim. Acta* **43** 1281
[21] Matsuda A, Nguyen V H, Daiko Y, Muto H and Sakai M 2010 *Solid State Ion.* **181** 180
[22] Eckert H, Yesinowski J P, Silver L A and Stolper E M 1988 *J. Phys. Chem.* **92** 2055
[23] Hayashi S, Yanagisawa M and Hayamizu K 1991 *Anal. Sci.* **7** 955
[24] Haile S M, Boysen D A, Chisholm C R I and Merie R B 2001 *Nature* **410** 910